BACK-REACTED SAPONITE IN JURASSIC MUDSTONES AND LIMESTONES INTRUDED BY A TERTIARY SILL, ISLE OF SKYE

S.J. KEMP, C.A. ROCHELLE AND R.J. MERRIMAN

British Geological Survey, Sir Kingsley Dunham Centre,

Keyworth, Nottingham, UK. NG12 5GG

sjk@bgs.ac.uk

Running Head: S. J. Kemp *et al.* Back-reacted saponite in Skye mudstones and limestones

ABSTRACT

The Lòn Ostatoin stream section, Trotternish Peninsula, Isle of Skye, exposes a sequence of Middle Jurassic mudstones and limestones which have been locally metasomatised by a transgressive sill of Tertiary age. Limestones in the sequence, including some previously reported as bentonite, have been altered to an unusual assemblage of grossular garnet and saponite clay. The mudstones also contain high proportions of saponite together with pyroxene and zeolites. Saponite also occurs within the basalt intrusion. Grossular and pyroxene represent artifacts of relatively high temperature assemblages that formed during an early phase of alteration. As the intrusion and adjacent altered country rocks cooled, lower temperature fluids flowed through a late set of contraction (micro)fractures. Back-reacted saponite, analcime and clinoptilolite were formed, possibly as alteration products of the unstable higher temperature minerals. The lower temperature mineral assemblage eventually sealed the late fracture system.

This paper highlights an important concept for the study of analogue sites used to investigate thermal effects on engineered liners or barrier host rocks for the landfill and radioactive-waste industries. This is that the original thermally altered mineral assemblage may be overprinted by later, lower temperature back-reactions. A detailed understanding of both processes is necessary in order to construct a sensible model for the thermal and mineralogical evolution of the site.

KEYWORDS: saponite, grossular, localised metasomatism, hydrothermal alteration, intrusion, Isle of Skye, X-ray diffraction, electron microscopy, geochemistry.

INTRODUCTION

Clay-rich rocks, including bentonite, mudstone and shale, are commonly employed as engineered liners, buffers and backfill, or as barrier host rocks in the landfill and radioactive-waste industries. Thermal alteration and shrinkage of the clay mineral components of such rocks affects their hydraulic integrity and ability to attenuate and buffer leachate components in landfills and, in particular radioactive-waste repositories. Where heat-emitting radioactive-wastes are involved, host rock clays may experience increases in temperature (possibly up to a maximum of 100°C) over extended timescales, whereas liners, buffers or backfills will experience higher temperatures (possibly in excess of 100°C) over shorter timescales (Horseman, 1997). Laboratory experiments (e.g. Cuevas *et al.*, 1997; Pusch *et al.*, 1996) are useful for studying the effects of increased temperatures over short timescales, but information over the longer timescales appropriate to performance assessment issues is more usefully obtained from 'natural analogues'. Such natural analogues provide valuable information into the overall understanding of processes, but do not in themselves identify sites where repositories might be sited.

Analogues for the thermal alteration of clay-rich materials used in repositories or in which repositories are excavated can be found in smectite-bearing Jurassic sedimentary rocks intruded by Tertiary dykes and sills on the Isle of

Skye, western Scotland. The emplacement of minor intrusions at liquidus temperatures of about 1100°C locally generated a high thermal gradient in the adjacent sedimentary rocks. Although peak temperatures generated at intrusive contacts are considerably higher than those expected in waste repositories, the 100 to 1000 year time taken for localised thermal gradients adjacent to thin dykes (<2.0 m wide) to decay to *c.*100°C appears to be within the time interval expected for heat dissipation around heat-emitting waste (e.g. Bishop & Abbott, 1995). Moreover, the smectite-rich mudrocks on Skye are analogous to clays which have been studied as host rocks for radioactive waste in Europe, e.g. the Belgian Boom Clay (Decleer *et al.*, 1983). The presence of bentonites within these mudstone sequences (e.g. Knox, 1977; Andrews, 1984; 1987) provides the additional prospect of identifying analogues that could be used to assess the thermal alteration of smectite-rich backfill materials. Importantly, the northernmost Jurassic outcrops on Skye have not been affected by thermal overprinting associated with the emplacement of the Cuillins and Red Hills plutons, which extends for no more than 15 km (Thrasher, 1992).

Although the patterns of mineral facies developed in thermal aureoles around major intrusions has been well documented (e.g. Winkler, 1967; Kerrick, 1991; Bucher & Frey, 1994), studies of the alteration associated with minor intrusions or of the low temperature (outermost) zones of aureoles around major intrusives are less numerous. Patterns developed in the low temperature zones of aureoles, referred to as ‘cryptic aureoles’ (Merriman & Frey, 1999),

indicate that smectite-rich clays undergo a systematic decrease in the proportion of smectite and an increase in the Reichweite ordering in mixed-layer illite/smectite (I/S) as the intrusive contact is approached (e.g. Nadeau & Reynolds, 1981). Smectite and I/S are absent and usually only muscovite-illite and chlorite are found in typical pelitic hornfelses developed in medium grade (hornblende-hornfels facies) aureole rocks. In some spotted hornfelses however, anomalously high illite crystallinity values have resulted from back-reactions associated with localised hydrothermal activity (Merriman & Frey, 1999). The few reported studies of contact effects on clays adjacent to minor intrusions also suggest that smectite proportions decrease and ordering increases in mixed-layer I/S as the intrusion is approached (Smart & Clayton, 1985; Bühmann, 1992). Organic maturity also increases in sedimentary rocks adjacent to minor intrusions, although Bishop & Abbott (1995) show that thermal effects are limited to zones up to 70% of dyke thickness from the contacts.

Here we describe the effects of a Tertiary intrusion on smectite-bearing mudstones and associated limestones in the Jurassic strata of northern Skye (Fig. 1). This work provides a description of a single natural analogue site, which was one of several investigated as part of a larger, partly European Community-funded programme studying natural analogues of the thermo-hydro-chemical and thermo-hydro-mechanical response of clay barriers (Pellegrini *et al.*, 1998).

GEOLOGICAL SETTING

Jurassic strata crop out over a wide area of Skye and offshore beneath much of the Sea of the Hebrides and the Minch. On the coast of northern Skye, outcrops around the margins of the Tertiary plateau basalts are in excess of 500 m thick. The succession was deposited in the Sea of the Hebrides Basin and is entirely marine or estuarine in origin with abundant fossils (Hudson, 1983). Preservation of almost the full extent of the Jurassic system and the most complete succession in Scotland, owes much to the protection of a thick capping of Tertiary plateau basalts. The middle Jurassic sediments examined in this study were laid down in an estuarine environment in deltas, mudflats and lagoons that varied from freshwater to brackish or rarely nearshore marine. In the upper part of the Middle Jurassic, the Great Estuarine Group is composed of sandstones, shales and some algal limestones, thin oil-shales and impure coals. Shales become more abundant in the overlying Staffin Bay Formation, particularly in the north of the island.

While the burial history of the Jurassic is not well known, slow and steady subsidence of the Sea of the Hebrides Basin is believed to have occurred through the Callovian, Oxfordian and lower Kimmeridgian (Sykes, 1975). Hudson & Andrews (1987) suggest a maximum depth of burial (Jurassic-Cretaceous) of less than 500 m, with the possible addition of up to 600 m of Tertiary lavas (Emeleus, 1983). Stable isotope data and burial history reconstructions (Hudson & Andrews, 1987) suggest that the maximum

temperature experienced by these rocks during burial diagenesis would have been in the order of 50°C. Uplift followed the cessation of Tertiary igneous activity (Hudson, 1983).

Tertiary volcanism on Skye, the result of magmatic doming and crustal rifting related to the opening of the North Atlantic, comprises three main elements (Brown *et al.*, 1969). Firstly, a sequence mainly formed of alkali olivine-basalts, which form extensive lava plateaus covering about 1000 km^2 and *c.*600 m in thickness. Secondly, the layered basic complex of the Cuillin Hills of coarsely crystalline products of tholeiitic magma, and thirdly, the post-Cuillin granitic complexes of the Red Hills.

Vertical or steeply inclined dykes of Tertiary age are present throughout Skye and adjacent islands (Richey, 1961; Anderson & Dunham, 1966). Apart from those closely associated with the major intrusive centres, the dykes generally trend between NNW-SSE and NW-SE and constitute a major regional swarm which extends over an area of 4000 km^2 from Lewis to Harris, through Skye to the Great Glen. Most of the dykes are basaltic and <2 m wide, but some reach 40 m in thickness, and in places may occupy up to 20% of the country rock outcrop.

LÒN OSTATOIN

The south-western bank of the Lòn Ostatoin stream [NG 4076 7268], Trotternish (Fig. 2), some 500 m inland from the coast road, exposes the type section of the upper part of the Kilmaluag Formation, stratigraphically the highest beds seen in this part of Skye (Andrews & Walton, 1990). The formation is here interpreted as a low-salinity, closed lagoon or coast-marginal lake (Hudson, 1980). Lagoonal sedimentation was mainly influenced by climate. Humid periods increased runoff, resulting in a clastic supply and the precipitation of carbonate muds which probably formed in a similar way to those from the Inner Hebrides Basin. Arid intervals allowed dolomitization and the periodic exposure of extensive mudflats (Andrews, 1985). Fossils in the Kilmaluag Formation are dominated by the ostracodes *Theriosynoecum* and *Darwinula*, the bivalve *Unio*, the gastropod *Viviparus* and the brachiopod *Cyzicus*, all of which are indicative of low salinity (Hudson, 1963).

The exposed sequence is generally composed of dark, weathered shales interbedded with argillaceous limestones and fine-grained sandstones (Fig. 3). Samples were removed from all the clay-rich beds (Beds 5, 7 and 9, Andrews, 1984) and in particular from the ‘white weathered top’ of the argillaceous limestone (Bed 8, Andrews, 1984). The latter has a white, soapy, fine-grained appearance that strongly resembles a bentonite. Detailed sample locations are

shown in Fig. 2. Throughout this paper, the samples have been assigned to the bed numbers delimited by Andrews (1984).

The sedimentary sequence is exposed in a 5 m high cliff on the south-western side of the stream where it is intruded by a sill-like sheet of microgabbro (Fig. 2). The beds have been deformed and tilted upwards at the south-eastern end of the exposure, presumably due to the vertical transgression of the mafic magma. On the north-west side of the exposure the intrusion lies horizontally within the sedimentary rocks, suggesting a single transgressive emplacement of the sheet. A xenolith of argillaceous limestone (Bed 8) is also seen in the exposure. Samples of the intrusion and limestone xenolith were also recovered for laboratory analysis.

Andrews (1984; 1985; 1987) also described a 'bentonite' from lower in the succession (Bed 4) as a conspicuous 50 mm thick pale grey-buff coloured soft clay with soapy texture and sharp upper and lower contacts with the surrounding shale. The lower half of the clay is silty and laminated on a millimetre scale. Some of the laminae are rich in winnowed ostracodes with *Cyzicus*, fish teeth and scales. The upper half of the bed is not silty but ostracodes are again present (Andrews, 1987). Andrews (1987) inferred a volcanogenic origin for the bed on the basis of the clay mineral assemblage that is predominantly smectite with subordinate vermiculite and illite. Because of the presence of silt grains and winnowed layers of ostracodes, he suggested that the bed represented a secondary bentonite, in this case terrestrial ash

redeposited in a lagoonal environment. No residual minerals, commonly described from bentonites e.g. feldspars, apatite, zircon or cristobalite were identified. Mg-vermiculite was interpreted as a Recent weathering product as none was detected in more deeply excavated samples. Andrews (1987) suggested two possible sources for the bentonite's precursor volcanic material, either the Bathonian-Bajocian volcanic complex of the Forties area of the North Sea, or volcanicity associated with North Atlantic rifting in the Rockall area. A further sample of Bed 4 was collected for analysis.

LABORATORY METHODS

The mineralogy of the samples was investigated using X-ray diffraction (XRD) analysis and both secondary electron scanning electron microscopy (SEM) and backscattered scanning electron microscopy (BSEM). Clay mineral assemblages were determined using a combination of XRD analysis of separated <2 μm fractions, and determinations of surface area, cation exchange capacity and exchangeable cation chemistry. The chemistry of certain phases was investigated using an electron microprobe. Further details of the analytical methodologies are given in Kemp & Rochelle (1998).

Dried samples were stage-crushed in short, 5 seconds bursts in the Cr-steel tema mill to pass a 1 mm sieve of which approximately 25 g was then hammer-milled to pass 0.2 mm.

Whole-rock XRD analyses were carried out on micronised, hammer-milled powders which were backloaded into standard aluminium sample holders. The <2 μm separates were isolated by gravity settling, then Ca-saturated, re-suspended and pipetted onto ceramic tiles in a vacuum apparatus to produce oriented mounts. XRD analysis was carried out using a Philips PW1700 series diffractometer equipped with a cobalt-target tube and operating at 45kV and 40mA. Diffraction data were analysed using Philips APD1700 software coupled to an International Centre for Diffraction Data (ICDD) database running on a DEC MicroVax 2000 micro-computer system. Whole-rock samples were scanned from 3-50° 2θ at 0.48° 2θ/minute. Clay mineralogy was determined after scanning the oriented samples as air-dry and glycol-solvated mounts and after heating the mounts to 375°C for 2 hours and 550°C for 2 hours. Each oriented mount was scanned from 1.5-32° 2θ at the same speed as the whole-rock samples. To differentiate vermiculite in the presence of smectite, Mg-saturated mounts were prepared and scanned as air-dry and directly applied-glycerol solvated mounts. In order to measure the *b* lattice parameter of clay minerals in selected samples, approximately 5 mg of <2 μm material was mounted on a zero-background silicon wafer substrate using a single drop of acetone. The mounts were scanned from 70-74° 2θ at a speed of 0.12° 2θ/minute.

2-ethoxyethanol (EGME) surface area determinations were carried out following a procedure based on that of Carter *et al.* (1965). Percent smectite in

the samples was calculated assuming pure smectite to have a surface area of approximately 800 m^2/g.

Cation exchange capacity (CEC) determinations were carried out using a $BaCl_2$/triethanolamine (pH 8.1) titration method based on that proposed by Bascomb (1964).

In addition, exchangeable cations were released from mineral phases by ammonium acetate and the leached solutions analysed for Ca, Mg, Na and K by inductively coupled atomic emission spectroscopy (ICP-AES) following the method detailed in Inglethorpe *et al.* (1993).

Determination of the major and trace element geochemistry for both the intrusion and the sedimentary rocks was carried out using sequential, fully automated wavelength-dispersive X-ray fluorescence spectrometers controlled by Philips X40 software. Glass beads were prepared by fusing the powdered sample with dried di–lithium tetraborate flux at approximately 1150°C. A lithium iodide releasing agent was added to the mixture before melting. Loss on ignition was calculated from the weight loss of 1 g of sample heated at 1050°C for 1 hour. Samples for trace element analysis were prepared by grinding the sample together with Elvacite for 45 minutes before pressing at 25 tons load into pellets.

Thin sections prepared from the intrusion samples were studied under the optical, petrographic microscope. Mudstone and limestone samples were also

examined by scanning electron microscope techniques using a Cambridge Instruments Stereoscan 250 and Leo 435VP in both scanning (SEM) and backscattered electron imaging (BSEI) modes with attached energy dispersive X-ray analyser (EDXA). These samples were resin–impregnated over a period of 1–2 weeks in order to minimise the shrinkage and disturbance of microtextures. Blue dye was added to the resin to aid the identification of microfractures, some of which were generated by clay shrinkage during thin section preparation. Samples imaged in the scanning mode were prepared by freeze drying.

Carbon-coated polished thin sections were also analysed using a Link Systems energy-dispersive X-ray analyser on a Cambridge Instruments Microscan 5 electron microprobe. The limits of detection for the microprobe are usually around 0.2 wt% oxide, but are higher where there are severe spectral interferences and may reach 1 wt% in the worst cases.

RESULTS

The intrusion

The margin of the intrusion, sampled close to the stream, is a fine-grained, aphyric basalt. It is composed of a randomly oriented framework of plagioclase laths (<0.5 mm), sub-ophitic clinopyroxene (<1 mm) and opaques (<0.1 mm) mostly composed of magnetite. No fresh olivine was observed,

although a few small (0.1-0.2 mm) iddingsite/clay pseudomorphs were found, indicating weathering of the original olivine. Brown clay minerals, identified as saponite by XRD, have replaced parts of the groundmass, which probably contained primary glass.

The interior of the intrusion, some 2 m from its basal contact, is an olivine microgabbro, coarser and possibly less evolved in composition than the marginal contact sample. It is composed of subhedral olivine (<1.5 mm, *c.*20%) with small inclusions of chrome spinel, subophitic clinopyroxene (<2 mm, *c.*35%), randomly oriented plagioclase (<0.5 mm, *c.*34%) and equant opaque grains (magnetite, *c.*1%). The olivine has been partially replaced by iddingsite along cracks and brownish, saponite (from XRD) replaces parts of the groundmass (*c.*10%).

Geochemical data (Tables 1 and 2) indicate that the intrusion represents a "within-plate" basalt with tholeiitic affinities that plots within the fractionation trend presented by Gibson (1990) for the Trotternish sill field (see Kemp & Rochelle, 1998 for full details).

Limestones

Samples from the argillaceous limestone (Bed 8) and the 'bentonite' (Bed 4) are composed of grossular garnet and smectite with calcite, albite, quartz, analcime and undifferentiated mica present in some samples. Equivalent smectite contents appear to decrease northwestwards along the outcrop from

32 to 21% (Table 3), away from the vertical part of the intrusion (Fig. 2). The smectite contents derived from surface area measurements, which includes a contribution from analcime, suggest that grossular generally forms >50% of the mineral assemblage. An example of a whole-rock XRD trace for the limestone is compared to grossular and smectite standard patterns in Fig. 4.

SEM examination reveals that both the Bed 8 and Bed 4 samples are composed of subhedral, occasionally euhedral, approximately 5-10 μm diameter grossular garnet crystals in a fine-grained clay matrix. The garnet occurs as isolated single crystals or clusters of up to six crystals and accounts for as much as 70% of a typical field of view (Fig. 5a-e). The crystals show dodecahedral and trapezohedral sections, are commonly cracked and often show corroded cores (Fig. 5b, d, e). Garnets from both beds have a grossular-like chemistry (Table 4) but those from Bed 4 contain a significant phosphorus content probably resulting from the presence of tiny apatite inclusions. [Large bone fragments and corroded, apatite-replaced bioclasts which may reach 250 μm in length were also observed (Fig. 5c)].

The clay matrix is composed of large, platy-crystal aggregates with curved edges reaching 10 μm in size (Fig. 5a, b, e). Patchy calcite cement and framboidal pyrite crystals were also observed in the matrix. The delicate curved crystal morphologies of the clay aggregates are typical of diagenetic smectites (cf. Nadeau, 1998). The absence of any garnet crystals overgrowing the flakes suggests that the clay post-dates the garnet (Fig. 5a, b). Moreover,

the corroded appearance of the garnet crystals suggests that they are not in stable equilibrium with the clay matrix. A limited number of electron microprobe analyses of the clay matrix in Bed 4 indicated an Mg, Ca (K) alumino-silicate chemistry (Table 4).

XRD analyses indicates that the clay mineralogy of Bed 8 and Bed 4 is dominated by smectite with possible vermiculite and illite. The smectite presents sharp basal peaks suggesting relatively thick and well-ordered clay crystallites. Rational spacings were recognised up to the d_{005} peak (Fig. 6) and the d_{060} peak (not shown) gives a spacing of 1.53 Å, indicating a trioctahedral smectite. The intense d_{001} peak together with the Mg-rich and trioctahedral nature of the clay matrix indicate that it is probably a saponite. Cation exchange sites, however, are dominated by divalent ions with Ca and Mg making up about 90% of the cations, in approximately equal proportions (Table 3). Vermiculite was tentatively identified on the basis of a 14.5 Å peak which is invariant after Mg-saturation and glycerol-solvation. No interlayered clay minerals, such as illite/smectite or chlorite/smectite were identified.

The core of the limestone xenolith has a similar mineralogy to the other limestone samples, comprising grossular and up to 13% smectite (Table 3). The exterior of the xenolith shows a more complex mineralogy of smectite (*c.*13%), analcime, diopside, K-feldspar and grossular. Mg (59%) is the predominant exchangeable cation in the xenolith core sample, Ca is next with 34%, and K and Na are present in small amounts (Table 3). The edge of the

limestone xenolith shows the development of a spheroidal texture. These are very fine-grained structures with a Ca, Fe-aluminosilicate chemistry. A patchy calcite cement together with occasional calcite bioclasts and corroded apatite grains appear to represent the original constituents of the limestone.

In the absence of data from unaltered sedimentary rocks in the part of the Lòn Ostatoin section studied, the geochemistry of the sedimentary rocks were compared to the standard North American Shale Composite (NASC) (Gromet *et al*., 1984). As shown in Fig. 7, the normalised patterns of the limestone and 'bentonite' are similar. They show considerable enrichment in Ca, P and Mn compared to NASC, and slight enrichment in Mg. Na and K are severely depleted together with slight depletion in Si, Ti and Al; Fe values are approximately similar to NASC. The sample from the limestone xenolith shows a similar pattern to the other limestone samples except for relative enrichment in Na and only slight depletion in K compared to NASC. In comparison with the surrounding mudstones, the trace elements Ba, Pb, Rb and Sr also appear depleted in the limestone.

Mudstones

The mudstones below the limestone (Beds 5 and 7) are predominantly fine-grained and laminated, with sporadic subrounded, silt-sized quartz, K-feldspar and albite grains in a clay matrix (Fig. 8a). Samples close to the intrusion contain pyroxene and one sample from the middle of Bed 7 also contains

minor grossular. The clay matrix of the mudstones is composed of smectite and illite with the occasional presence of vermiculite. The sharp smectite XRD basal peaks, a d_{060} peak spacing of 1.53 Å and an intense d_{001} peak indicate that the smectite is likely to be a saponite. Surface areas suggest smectite contents in the range 15 to 43% (Table 3). Exchangeable cations generally comprise a mixture of Ca, Mg and Na with little K (Table 3). Analcime is developed as a patchy cement often following the sedimentary lamination (Fig. 8a), as a vein-fill and as a replacement for the cores of bioclasts whose exteriors are often phosphatised (Fig. 8b). Mica flakes are generally unorientated and often replaced by Fe, Ti-oxides. Veins of coarse-grained clinoptilolite and analcime are commonly fractured and trend perpendicular to the lamination. Cross-cutting veins of analcime suggest they were formed later than those filled with clinoptilolite (Fig. 8c). Under the optical microscope the clay fabric is mostly parallel with the bedding lamination. However, around some bioclasts the clay fabric is partly radial and may indicate local nucleation of clay crystals in response to contact alteration.

Geochemically, these mudstones are enriched in Na and Mg and to a lesser extent K, Fe, and P compared to NASC (Fig. 9). They are severely depleted in Ca and to a lesser extent Si, whereas Al, Ti and Mn are approximately similar to NASC values.

The silty/sandy, laminated mudstones of Bed 9 above the limestone bed show similar features to the mudstones beneath the limestone. They are generally composed of smectite (17-33%), quartz, feldspar, analcime, clinoptilolite and 'mica'. Their <2 μm fractions reveal a saponite and illite clay mineralogy. Samples containing analcime have Na-dominant cation exchange capacities (e.g. high Na (46%), minor Ca and Mg (both 26%)) while those that lack analcime are predominantly composed of Ca (44%) and Mg (45%) (Table 3). The silty laminae, however, are composed of subrounded to subangular quartz, K-feldspar, rare albite, Fe, Ti-oxides with a clay matrix cemented by clinoptilolite (Fig. 8d). Euhedral K-feldspar overgrowths are common, particularly on albite grains. Rare corroded pyrite cubes were observed in the clinoptilolite cement.

Like the other mudstones, Bed 9 is similarly enriched in Mg and Na but depleted in Ca, K and P relative to NASC (Fig. 9). Trace elements Rb, Sr, Ba and Pb are enriched in these mudstones compared to the limestone.

DISCUSSION

Limestones

Both the 'white weathered limestone' (Bed 8) and 'bentonite' (Bed 4) exhibit an unusual, previously undescribed mineralogy, comprising largely grossular garnet, saponite and vermiculite. In the case of Bed 4, such a mineralogy combined with the low concentrations of characteristic immobile trace elements such as Zr, and a lack of residual minerals or cristobalite do not support a volcanogenic origin. The lack of grossular and the different geochemistry of the mudstones above and below Bed 8 indicate that both Bed 8 and Bed 4 differed significantly from the surrounding mudstones. Their Ca-dominated geochemistry, fossil-content and light colouration suggest that they were both originally impure limestones which were subjected to thermal alteration and metasomatism.

Grossular garnet ($Ca_3Al_2Si_3O_{12}$) is typically found in both thermally and regionally metamorphosed impure calcareous rocks, and in rocks which have undergone calcium metasomatism. It has previously been found in metamorphosed marls and shales and may result from the replacement of earlier formed wollastonite (Deer *et al.*, 1992). Other occurrences include zeolite-bearing vesicles in metamorphosed basaltic lavas, associated with granite pegmatite pneumatolysis, highly metamorphosed layered complexes as

an alteration of anorthite and hydrothermally altered marly rocks (Abad *et al.*, 2003). Laboratory experiments with CaO-Al_2O_3-SiO_2 systems in H_2O-CO_2 fluids (Tracy & Frost, 1991) suggest that anhydrous grossular may be synthesized at a wide range of temperatures (300 to 900°C). Grossular is stable across the entire range of H_2O-CO_2 fluid compositions at 1000 bars but is unstable in CO_2-rich fluids at lower pressures of 500 bars.

The shallow burial of the Jurassic limestones and close proximity of a transgressive sill strongly suggest that the abundant grossular identified in the exposures at in Lòn Ostatoin was formed by localised metasomatic alteration, driven by the infiltration of magmatic fluids (Barton *et al.*, 1991). The small (approximately 5-10 μm), uniform size-distribution and often euhedral nature of the garnet crystals suggests that they crystallised relatively quickly, probably in a single event at the lower end of the increased temperature range. The significant phosphorus content of the garnets in Bed 4 provides further evidence for local metasomatism of the limestones. Phosphate was probably mobilized from pre-existing bone fragments and fish teeth in the unaltered limestones (Andrews, 1987). Unfortunately, the absence of unaltered limestone samples precludes chemical comparison and further comment upon the nature of the fluids.

In studies of high temperature metasomatised limestones, Einaudi *et al.* (1981) identified assemblages of garnet, pyroxene, pyroxenoids and idocrase as being characteristic of anhydrous skarns. Reduced skarns are typified by grossular

and sub-calcic garnets with Fe-rich clinopyroxenes. Whilst pyroxene was identified in the margin of the limestone xenolith, garnet is the only characteristic skarn mineral commonly identified in the Lòn Ostatoin limestones. It would therefore appear that either the pyroxene, pyroxenoids and idocrase have been selectively removed by later hydrous alteration or that the primary metasomatism occurred at a relatively low temperature where garnet crystallised but other skarn minerals were unstable. The cracked morphology and corroded cores of the garnets suggest a later phase of fluid-alteration but no evidence for the pre-existence of other high temperature minerals was observed.

Although smectites are generally considered to be low temperature minerals, saponite may form at 300-500°C during basalt alteration in different environments (Kristmansdottir, 1979; Güven, 1988) and >500°C in experimental systems (Kuchta & Fajnor, 1988). Wilson *et al.* (1968) describe the development of saponite during medium-high grade metamorphism of Dalradian limestones in north-east Scotland. The post-garnet growth of saponite in the Lòn Ostatoin limestones provides further evidence for a later phase of fluid alteration where temperatures probably did not exceed 500°C.

Assemblages of saponite and vermiculite have often been described from locations associated with mafic volcanism but invariably occur in vein and amygdale fillings. April & Keller (1992) identified saponite and vermiculite in amygdales in the Granby Basaltic Tuff in the Connecticut Valley and noted the

similarity in their chemistry but different layer charge. The authors suggested that both clay minerals precipitated from solutions generated by the hydrothermal alteration of the basaltic tuff. Garvie & Metcalfe (1997) also describe saponite with a small proportion of possible vermiculitic material from veins cutting a hydrothermally altered andesite at Builth Wells, Wales. They indicated that the clays were deposited from ascending Mg-rich, low-pH fluids expelled from underlying marine mudrocks. Cowking *et al.* (1983) also describe veins of saponite cutting basalt in a quarry at Orrock, Fife. Saponite, and variable amounts of corrensite with chlorite, are developed in late veins caused by hydrothermal alteration of contact metamorphosed marly rocks in the Betic Cordillera of Spain (Abad *et al.*, 2003). Saponite is also widely developed by low temperature hydrothermal alteration of oceanic basaltic crust (Alt, 1999).

Barton *et al.* (1991) suggest that metasomatism in and around mafic intrusions is largely due to the circulation of external fluids, often overprinting more localised magmatic alteration. Alt *et al.* (1986) describe well developed zoning and widespread retrograde effects due to extensive seawater circulation. Such mafic marine systems produce uniquely large-scale alterations due to the unlimited supply of seawater and constant supply of new magma. In ridge environments, downward zoned sequences of increasingly higher temperature assemblages have been identified (e.g. Schiffman & Smith, 1988; Alt, 1999). The deeper sequences are characterised by Na ± Ca metasomatism whereas at shallower depths Mg-metasomatism predominates.

Such a zonation is explained by the ingress and near surface reaction with Mg-bearing seawater while the deeper alteration represents reaction with Mg-depleted seawater.

Given the original location of the rocks adjacent to a marine setting, it would therefore seem plausible that saponite (and vermiculite) at Lòn Ostatoin developed as a result of low temperature alteration by Mg-bearing seawater. The precursor mineralogy of the limestone probably consisted of anhydrous skarn minerals such as garnet, pyroxene, pyroxenoids and idocrase, but only grossular garnet has survived. The corroded and embayed grossular crystals show typical disequilibrium texture suggesting retrogression. They are enclosed by saponite crystals showing the characteristic curved 'corn-flake' morphologies of diagenetic smectites (Fig. 5). Pervasive development of saponite crystals suggest that low temperature alteration was extensive and continued for some time. However, saponite concentration decreases northwestwards along the outcrop (Fig. 2), suggesting that back-reaction was most vigorous close to the vertical part of the intrusion. Moreover, the presence of saponite in the groundmass of the intrusion provides clear evidence that Mg-bearing fluids caused post-magmatic alteration of the basalt.

Mudstones

Close to the intrusion, the mudstone beds show mineral assemblages indicative of high temperature thermal alteration. In particular, samples close to the vertical part of the intrusion contain pyroxene which has a crystallisation temperature of approximately 900°C (Deer *et al.*, 1992).

The matrix of the mudstones is dominated by smectite with traces of illite (Assemblage 2 of Andrews, 1987). It is probable that the pre-intrusion, diagenetic clay assemblage of the mudstones was dominated by dioctahedral smectite, consistent with relatively shallow, approximately 1 km burial (Hudson & Andrews, 1987). *b* lattice parameter measurements show the presence of trioctahedral smectite, suggesting that this diagenetic smectite was subsequently altered to saponite. Several other features also suggest that the mudstones have undergone metasomatism by Mg-bearing fluids. Firstly, most Jurassic mudstones in the UK are diagenetic in terms of their maturity, and lithologies similar to those found on Skye usually contain appreciable proportions of kaolinite (Merriman & Kemp, 1996). However, no kaolinite was identified in any of the samples examined. Kaolinite dehydroxylates at approximately 550°C in the laboratory (Moore & Reynolds, 1997), but breaks down in the presence of potassium to form illite and/or chlorite at temperatures of only 140-180°C where it forms a minor component of mudstones or shales (Hoffman & Hower, 1979). Even low temperature metasomatism would therefore remove any kaolinite present in the mudstones. Secondly, the

relatively high proportion of the exchangeable cation chemistry formed by Mg is greater than that reported from UK Jurassic mudstones (e.g. Perrin, 1971). Thirdly, vein-fills and matrix cements composed of analcime and zeolites were clearly formed by precipitation from relatively low temperature fluids. The Na and Mg-enriched geochemistry of the mudstones provides additional evidence for alteration, reflecting the low temperature hydrothermal growth of analcime, clinoptilolite and saponite. Furthermore, as noted for the limestones, smectite contents decrease in general away from the vertical part of the intrusion suggesting more vigorous back-reaction close to that contact.

The original sedimentary lamination is still visible in many of the mudstone samples, but close to the vertical part of the sill, the micro-fabric shows a high angle extinction indicative of the deformation induced by intrusion. In places this fabric is developed to the point of almost imparting a crude cleavage. Fracturing, however, is widespread and may reflect hydrofracturing, thermal shock or thermal contraction during the emplacement of the sill. These fractures have later been sealed by analcime and clinoptilolite cements. Textural relationships suggest that clinoptilolite precipitated before the analcime. Ranges of precipitation temperatures have been published for such phases, but temperatures of the order of 150°C for analcime (Wiersema & Thompson, 1996) and 100°C for clinoptilolite (Iijima & Utada, 1971) suggest that both minerals were formed by relatively low temperature fluids. Zeolite crystallisation may reflect the waning thermal influence of the intrusion

analogous to the ‘ageing’ of hydrothermally altered oceanic volcanic rocks (Alt, 1999).

Alteration history

Field observations and laboratory analysis enable a tentative model to be constructed for the deposition and subsequent alteration of the sequence exposed in Lòn Ostatoin.

The mudstones and limestones were deposited as part of the Jurassic sedimentary sequence in an estuarine environment of deltas, mudflats and lagoons which varied from freshwater to brackish or rarely nearshore marine. The sediment supply was composed of fine-grained quartz, feldspar, mica flakes and shell fragments together with the clay minerals smectite, illite and almost certainly kaolinite. Subsequent sedimentation buried the sequence to a depth of approximately 0.5 km during which time strata became lithified and developed a weak sedimentary fabric.

Tertiary igneous activity due to rifting during the opening of the North Atlantic resulted in further burial of the mudstone beneath approximately 0.5 km of lavas and emplacement of a basaltic transgressive sill, which probably represents part of the lava feeder system. Heat from the sill and tectonic stresses associated with its emplacement caused initial dehydration, cracking and hydrofracturing of the adjacent mudstone sequence. As magmatic fluids and superheated pore-waters moved through both the mudstones and

limestones, relatively high temperature mineral assemblages containing pyroxene and grossular garnet formed close to the intrusion. Although no longer present, pyroxenoids and idocrase may also have crystallised locally. When the intrusion and adjacent altered country rocks cooled, a late set of contraction joints and (micro)fractures formed. These provide conduits for cooler fluids, probably consisting of seawater and late magmatic fluids to move through the basalt and the adjacent contact altered mudstones and limestones. Saponite, analcime and clinoptilolite were formed as back-reaction products of the early-formed, anhydrous, higher temperature minerals. Grossular garnets in the limestones, although corroded by such fluid interaction, remained essentially as formed. The back-reacted, low temperature mineral assemblage eventually sealed the contractional fracture system that provided access for the late fluids.

The peak temperatures experienced by the rocks at Lòn Ostatoin were well in excess of those expected adjacent to any likely repository for heat-emitting radioactive wastes, as is the extent of the alteration. However, the low temperature processes identified at Lòn Ostatoin present significant implications for engineered liners or barriers for the waste (especially radioactive-waste) industries. The analogous emplacement of heat-emitting radioactive wastes could similarly effect dehydration, contraction and fracturing of host rock clays and engineered bentonite liners, buffers and backfills during the initial ‘hot’ phase, shortly after waste emplacement. As the waste canisters cool, later movement of low-temperature pore-fluids along

these fractures would then lead to rehydration of the backfill and sealing of the fractures by the development of authigenic, highly sorptive species. Any such 'self-sealing' mechanism would be beneficial in terms of waste containment, especially if it occurred prior to the expected degradation of the waste canisters.

We are unaware of any experimental work on the use of a saponite buffer for radioactive waste containment. Saponite would be expected to show different dehydration behaviour from commercial bentonite (Na-smectite) used in most experimental buffers. Products of saponite dehydration reactions include mixed-layer saponite/chlorite (corrensite) and vermiculite/chlorite minerals, followed by chlorite as reactions progress to higher temperatures (Merriman & Peacor, 1999). Although the mudstones at Lòn Ostatoin were not originally saponite-bearing, they provide a useful analogue for waste containment in an environment where low-temperature sea-water has the potential to access a dehydrated and fractured bentonite buffer system.

CONCLUSIONS

The Lòn Ostatoin section exposes a sequence of locally metasomatised mudstones and limestones that have experienced relatively high temperatures associated with the emplacement of a Tertiary sill. Clay minerals and zeolites present formed after cooling by back-reaction due to interaction with Mg-bearing fluids and are not related to the original sedimentary mineralogy. This unusual mineral assemblage highlights an important concept for other potential analogue sites, namely that the cooling and contractional fracturing of any rock system allows low temperature fluids to access minerals formed at a higher temperature and promote back-reactions.

ACKNOWLEDGMENTS

The authors wish to thank Jonathan Pearce and Vicky Hards (BGS) for their assistance with mineralogical analysis. This work forms part of a larger, partly EC funded project (DG XII, contract F14W-CT95-0014), studying natural analogues of the thermo-hydro-chemical and thermo-hydro-mechanical response of clay barriers. The authors are grateful to Richard April and Roland Pusch for their constructive and helpful reviews. This paper is published with the permission of the Executive Director, British Geological Survey (NERC).

REFERENCES

Abad, I., Jimenez-Millan, J., Molina, J.M., Nieto, F. & Vera, J.A. (2003) Anomalous reverse zoning of saponite and corrensite caused by contact metamorphism and hydrothermal alteration of marly rocks associated with subvolcanic bodies. *Clays and Clay Minerals* **51(5)**, 543-554.

Alt, J.C. (1999) Very low-grade hydrothermal metamorphism of basic igneous rocks. Pp 169-201 in: *Low Grade Metamorphism*. (M. Frey & D. Robinson, editors). Blackwell, Oxford.

Alt, J.C., Honnorez, J., Laverne, C. & Emmermann, R. (1986) Hydrothermal alteration of a 1km section through the upper oceanic crust, deep sea drilling project hole 504B; Mineralogy, chemistry, and evolution of seawater-basalt interactions. *Journal of Geophysical Research* **91**, 10309-10335.

Anderson, F.W. & Dunham, K.C. (1966) *The Geology of Northern Skye*. Memoir of the Geological Survey of Scotland, HMSO.

Andrews, J.E. (1984) *Aspects of sedimentary facies and diagenesis in limestone-shale formations of the (Middle Jurassic) Great Estuarine group, Inner Hebrides.* PhD thesis, Univ. Leicester, UK.

Andrews, J.E. (1985) The sedimentary facies of a late Bathonian regressive episode: the Kilmaluag and Skudiburgh Formations of the Great Estuarine Group, Inner Hebrides, Scotland. *Journal of the Geological Society of London* **142**, 1119-1137.

Andrews, J.E. (1987) Jurassic clay mineral assemblages and their post-depositional alteration: Upper Great Estuarine Group, Scotland. *Geological Magazine* **124**, 261-271.

Andrews, J.E. & Walton, W. (1990) Depositional environments within Middle Jurassic oyster-dominated lagoons: an integrated litho-, bio- and palynofacies study of the Duntulm Formation (Great Estuarine Group, Inner Hebrides). *Transactions of the Royal Society of Edinburgh: Earth Sciences* **81**, 1-22.

April, R.H. & Keller, D.M. (1992) Saponite and vermiculite in amygdales of the Granby basaltic tuff, Connecticut Valley. *Clays and Clay Minerals* **29**, 31-39.

Barton, M.D., Ilchik, R.P. & Marikos, M.A. (1991) Metasomatism. Pp 320-350 in: *Contact Metamorphism*. (D.M. Kerrick, editor), Reviews in Mineralogy, Mineralogical Society of America **26**.

Bascomb, C.L. (1964) Rapid method for the determination of cation exchange capacity of calcareous and non-calcareous soils. *Journal of the Science of Food and Agriculture* **15**, 821-823.

Bishop, A. N. & Abbott, G. D. (1995) Vitrinite reflectance and molecular geochemistry of Jurassic sediments: the influence of heating by Tertiary dykes (northwest Scotland). *Organic Geochemistry* **22**, 165-177.

Brown, G.M. (1969) *The Tertiary igneous geology of the Isle of Skye*. Geologists Association Guide No. 13, Benham and Company Ltd., Colchester.

Bucher, L. & Frey, M. (1994) *Petrogenesis of Metamorphic Rocks*, 6th edition. Springer-Verlag. Berlin, Heidelburg.

Bühmann, C. (1992) Smectite-to-illite conversion in a geothermally and lithologically complex Permian sedimentary sequence. *Clays and Clay Minerals* **40**(1), 53-64.

Carter, D.L., Heilmen, M.D. & Gonzalez, F.L. (1965) Ethylene glycol monoethyl ether for determining surface area of silicate minerals. *Soil Science* **100**, 356-360.

Cheng, W., Greenwood, H.J., Hu, H. & Frost, D.C. (1990) XRD and XPS analyses of the grossular-hydrogrossular series. *Canadian Mineralogist* **28**, 87-91.

Cuevas, J., Villar, M.V., Fernández, A.M., Gómez, P. & Martin, P.C. (1997) Pore waters extracted from compacted bentonite subjected to simultaneous heating and hydration. *Applied Geochemistry* **12**, 473-481.

Cowking, A., Wilson, M.J., Tait, J.M. & Robertson, R.H.S. (1983) Structure and swelling of fibrous and granular saponitic clay from Orrock quarry, Fife, Scotland. *Clay Minerals* **18**, 49-64.

Decleer, J., Viaene, W. & Vandenberge, N. (1983) Relationships between chemical, physical and mineralogical characteristics of the Rupelian Boom Clay, Belgium. *Clay Minerals* **18**, 1-10.

Deer, W.A., Howie, R.A., & Zussman, J. (1992) *An Introduction to the Rock Forming Minerals - 2nd edition*. Longman.

Emeleus, C.H. (1983) Tertiary igneous activity. Pp. 357-397 in: *Geology of Scotland*, (G.Y. Craig, editor). Scottish Academic Press.

Einaudi, M.T., Meinert, L.D. & Newberry, R.J. (1981) Skarn deposits. *Economic Geology* 75th Anniversary Volume, 327-391.

Garvie, L.A.J. & Metcalfe, R. (1997) A vein occurrence of co-existing talc, saponite, and corrensite, Builth Wells, Wales. *Clay Minerals* **32**, 223-240.

Gibson, S.A. (1990) The geochemistry of the Trotternish sills, Isle of Skye: crustal contamination in the British Tertiary Volcanic Province. *Journal of the Geological Society* **147**, 1071-1081.

Gromet, L.P., Dymek, R.F., Haskin, L.A. & Korotov, R.L. (1984) The "North American shale composite": Its compilation, major and trace element characteristics. *Geochimica et Cosmochimica Acta* **48**, 2469-2482.

Güven, N. (1988) Smectites. Pp. 497-559 in: *Hydrous Phyllosilicates (exclusive of micas),* (S.W. Bailey, editor), Reviews in Mineralogy, Mineralogical Society of America, Washington DC **19**.

Hoffman, J. & Hower, J. (1979) Clay mineral assemblages as low grade metamorphic geothermometers: application to the thrust faulted disturbed belt of Montana, USA. Pp. 55-79 in: *Aspects of Diagenesis,* (P.A. Scholle & P.R. Scluger, editors), SEPM Special Publication **26**.

Horseman, S.T. (1997) Thermal aspects of performance assessment for HLW disposal in clays and mudrocks. *British Geological Survey Technical Report* **WE/97/36R**

Hudson, J.D. (1963) The recognition of salinity-controlled mollusc assemblages in the Great Estuarine Series (Middle Jurassic) of the Inner Hebrides. *Palaeontology* **6**, 318-326.

Hudson, J.D. (1980) Aspects of brackish-water facies and faunas from the Jurassic of north-west Scotland. *Proceedings of the Geological Association* **91**, 99-105.

Hudson, J.D. (1983) Mesozoic sedimentation and sedimentary rocks in the Inner Hebrides. *Proceedings of the Royal Society of Edinburgh* **83B**, 47-63.

Hudson, J.D. & Andrews, J.E. (1987) The diagenesis of the Great Estuarine group, Middle Jurassic, Inner Hebrides, Scotland. Pp. 51-78 in: *Diagenesis of sedimentary sequences*, (J.D. Marshall, editor). Special Publication of the Geological Society, London **36**.

Iijima, A. & Utada, M. (1971) Present-day zeolitic diagenesis of the Neogene geosynclinal deposits of the Niigata oil field, Japan. Pp. 342-349 in: *In Molecular sieve zeolites I. American Chemistry Society Advanced Chemistry Series* **101**.

Inglethorpe, S.D.J., Morgan, D.J., Highley, D.E. & Bloodworth, A.J. (1993) Industrial Minerals Laboratory Manual: Bentonite. *British Geological Survey Technical Report* **WG/93/20**

Kemp, S.J. & Rochelle, C.A. (1998) A mineralogical, geochemical, petrographic and physical testing study of the thermal alteration of smectite-bearing mudstones from the Isle of Skye, Inner Hebrides. (I) Lùb Score, below Bealach Iochdarach. *British Geological Survey Technical Report* **WG/98/3R**

Kerrick, D.M. (1991) Overview of Contact-Metamorphism. Pp. 1-12 in: *Contact Metamorphism.*, (D.M. Kerrick, editor). Reviews in Mineralogy, Mineralogical Society of America **26**.

Knox, R.W.O'B. (1977) Upper Jurassic pyroclastic rocks in Skye, west Scotland. *Nature*, **265**, 323-324.

Kristmansdottir, H. (1979) Alteration of basaltic rocks by hydrothermal activity at 100-300°C. *Proceedings of the International Clay Conference, Oxford*, 359-367.

Kuchta, L'. & Fajnor, V.S. (1988) Optimal conditions for hydrothermal synthesis of saponite. *Chemistry Papers* **42**, 339-345.

Merriman, R.J. & Frey, M. (1999) Patterns of very low-grade metamorphism in metapelitic rocks. Pp. 61-107 in: *Low Grade Metamorphism*. (M. Frey, M. & D. Robinson, editors). Blackwell, Oxford.

Merriman, R.J. & Kemp, S.J. (1996) Clay minerals and sedimentary basin maturity. *Mineralogical Society Bulletin*, **111**, 7-8.

Moore, D.M. & Reynolds, R.C. (1997) *X-Ray Diffraction and the Identification and Analysis of Clay Minerals, Second Edition.* Oxford University Press, New York.

Nadeau, P. H. (1998) An experimental study of the effects of diagenetic clay minerals on reservoir sands. *Clays and Clay Minerals* **46**(1), 18-26.

Nadeau, P. H. & Reynolds Jr., R. C. (1981) Burial and contact metamorphism in the Mancos shale. *Clays and Clay Minerals* **29**(4), 249-259.

Pellegrini, R., Horseman, S., Kemp, S.J., Rochelle, C., Boisson, J.Y., Lombardi, S., Bouchet, A. and Parneix, J.C. (1998). Natural analogues of the

thermo-hydro-chemical and thermo-hydro-mechanical response of clay barriers. *Final Report EC contract FI-4W/CT95/0014.*

Perrin, R.M.S. 1971. *The Clay Mineralogy of British Sediments,* Mineralogical Society, London.

Pusch, R., Karnland, O. & Sandén, T. (1996) Final report on physical test program concerning Spanish clays (saponites and bentonites). *Empresa Nacional de Residuos Radiactivtivos, S.A. (ENRESA) Report* **02/96**.

Richey, J.E. (1961) *Scotland: The Tertiary Volcanic Districts (Third Edition).* British Regional Geology, HMSO.

Schiffman, D. & Smith, B.M. (1988) Petrology and oxygen isotope geochemistry of a fossil seawater hydrothermal system within the Soten Graben, northern Troodos Ophiolite, Cyprus. *Journal of Geophysical Research* **93**, 4612-4624.

Smart, G. & Clayton, T.C. (1985) The progressive illitization of interstratified illite-smectite from carboniferous sediments of northern England and its relationship to organic maturity indicators. *Clay Minerals* **20**(4), 455-466.

Sykes, R.M. (1975) The stratigraphy of the Callovian-Oxfordian (Middle-Upper Jurassic) in northern Scotland. *Scottish Journal of Geology* **11**, 51-78.

Thrasher, J. (1992) Thermal effect of the Tertiary Cuillins intrusive complex in the Jurassic of the Hebrides: an organic geochemical study. Pp. 35-49 in:

Basins on the Atlantic Seaboard: Petroleum Geology, Sedimentology, and Basin Evolution. (J. Parnell, editor). Special Publication of the Geological Society, London **62**.

Tracy, R.J. & Frost, B.R. (1991) Phase equilibria and thermobarometry of calcareous, ultramafic and mafic rocks, and iron formations. Pp. 207-280 in: *Contact Metamorphism*. (D.M. Kerrick, editor). Reviews in Mineralogy, Mineralogical Society of America **26**.

Wiersema, G.S. & Thompson, R.W. (1996) Nucleation and crystal growth of analcime from clear aluminosilicate solutions. *Journal of Materials Chemistry* **6**(10), 1693-1699.

Wilson, M.J., Bain, D.C. & Mitchell, W.A. (1968) Saponite from the Dalradian meta-limestones of North-East Scotland. *Clay Minerals* **7**, 343-349.

Winkler, H.G.F. (1967) *Petrogenesis of metamorphic rocks*, 2nd edition. New York: Springer-Verlag.

Table 1.

Bed	Sample	SiO_2	TiO_2	Al_2O_3	Fe_2O_3t	MnO	MgO	CaO	Na_2O	K_2O	P_2O_5	SO_3	Cr_2O_3	SrO	LOI	Total
Intrusion (contact)	CA67	46.74	1.58	15.37	11.03	0.16	7.54	10.70	3.04	0.21	0.15	0.3	0.04	0.04	3.25	100.15
Intrusion (core)	CA68	43.99	1.13	11.09	12.82	0.18	18.45	7.47	1.66	0.22	0.11	0.1	0.25	0.02	2.51	100.00
9 (base)	CA18	56.07	0.77	15.15	7.33	0.07	7.75	2.43	2.01	2.70	0.08	0.0	0.02	0.14	4.68	99.20
8 (top)	CA13	42.13	0.71	13.16	8.09	0.35	10.47	18.79	0.28	0.82	0.50	0.0	0.03	0.03	4.46	99.82
8 (top/middle)	CA17	38.96	0.67	14.31	7.70	0.30	4.47	29.54	0.08	0.17	0.78	0.0	0.02	0.02	2.66	99.68
8 (xenolith)	CA10	49.78	0.63	14.50	7.68	0.21	5.29	12.22	3.54	2.53	0.32	0.0	0.03	0.05	3.32	100.10
7 (top)	CA14	54.45	0.83	17.61	8.10	0.07	4.44	1.40	2.91	5.65	0.12	0.0	0.02	0.05	4.00	99.65
5 (top)	CA15	53.45	0.91	17.67	8.06	0.06	3.30	1.08	4.20	5.13	0.26	0.0	0.02	0.03	5.38	99.55
4	CA32	28.30	0.55	10.11	6.44	0.28	5.40	34.06	0.05	0.51	1.53	0.1	0.01	0.10	12.58	100.02

Note: Fe_2O_3t= total iron

Table 2.

Bed	Sample	Rb	Sr	Y	Zr	Nb	Ba	Pb	La	Ce	Nd	Th	U
Intrusion (contact)	CA67	3	365	18	102	3	64	<1	8	22	15	<1	<1
Intrusion (core)	CA68	4	215	13	74	3	469	<1	7	12	16	<1	1
9 (base)	CA18	87	1049	12	146	20	1003	16	34	74	34	8	4
8 (top)	CA13	21	265	20	158	17	350	5	32	69	28	6	3
8 (top/middle)	CA17	11	198	51	120	19	197	<1	59	116	52	7	1
8 (xenolith)	CA10	56	400	20	138	17	592	7	38	76	35	6	4
7 (top)	CA14	136	375	16	122	20	1088	18	39	74	37	7	2
5 (top)	CA15	126	238	31	171	22	984	18	52	111	54	8	5
4	CA32	41	749	26	105	15	296	3	36	56	24	5	7

Table 3.

Bed	Sample	Surface area analysis		Exchangeable cations (meq/100g) [%]					CEC
		(m^2/g)	%smectite	Mg	Ca	Na	K	Total	(meq/100g)
9 (base)	CA18	264.5	33	10.76 [45]	10.60 [44]	1.98 [8]	0.60 [3]	23.94	na
9 (base)	CA23	138.1	17	6.76 [26]	6.86 [26]	12.18 [46]	0.45 [2]	26.25	na
8 (top)	CA13	258.5	32	8.15 [44]	9.07 [49]	1.07 [6]	0.12 [1]	18.41	46.8
8 (top/middle)	CA17	111.4	14	4.72 [46]	4.82 [47]	0.54 [5]	0.08 [1]	10.16	na
8 (base)	CA25	250.0	31	8.67 [29]	16.49 [55]	3.34 [11]	1.51 [5]	30.01	na
8 (xenolith core)	CA11	104.2	13	6.06 [59]	3.52 [34]	0.70 [7]	0.07 [1]	10.35	na
8 (xenolith contact)	CA12	99.9	13	5.38 [38]	4.96 [36]	3.65 [26]	0.09 [1]	13.94	na
7 (middle)	CA19	219.7	27	4.22 [16]	17.77 [69]	2.83 [11]	0.83 [3]	25.65	na
7 (middle)	CA26	346.9	43	na	na	na	na	na	48.1
5 (top)	CA15	122.6	15	7.26 [34]	5.87 [28]	6.97 [33]	0.99 [5]	21.09	na
4	CA32	169.2	21	na	na	na	na	na	na

Note: na = not analysed

Table 4.

Bed	**8**	**4**	**4**
Phase	**Garnet**	**Garnet**	**Saponite**
No. analyses	15	20	6
SiO_2	38.75 (0.53)	37.81 (0.41)	40.06 (1.22)
TiO_2	0.52 (0.26)	0.81 (0.28)	0.26 (0.06)
Al_2O_3	16.72 (2.19)	16.37 (1.64)	8.91 (0.46)
Cr_2O_3	nd (-)	nd (-)	nd (-)
FeO	6.48 (2.75)	6.17 (1.95)	9.58 (1.47)
MnO	0.44 (0.34)	0.44 (0.15)	0.29 (0.05)
MgO	0.50 (0.35)	1.51 (0.45)	15.73 (1.87)
CaO	36.20 (0.67)	35.56 (0.69)	7.37 (3.21)
Na_2O	0.24 (0.05)	0.22 (0.05)	0.32 (0.05)
K_2O	0.28 (0.29)	0.35 (0.14)	1.14 (0.61)
P_2O_5	0.28 (0.03)	0.70 (0.22)	0.87 (0.29)
Total	99.49	99.69	84.34
Si	6.03	5.89	6.93
Ti	0.06	0.10	0.03
Al	3.07	3.00	1.82
Cr	nd	nd	nd
Fe	0.84	0.80	1.39
Mn	0.06	0.06	0.04
Mg	0.12	0.35	4.05
Ca	6.04	5.93	1.37
Na	0.07	0.06	0.11
K	0.06	0.07	0.25
P	0.04	0.09	0.13
Total	16.38	16.36	16.12
No. O, OH	24	24	24

Note: nd = not detected

TABLES AND FIGURES

Table 1. Summary of major element XRF analyses (%) including loss on ignition (LOI).

Table 2. Summary of trace element XRF analyses (ppm).

Table 3. Summary of surface area, cation exchange capacity and exchangeable cation determinations.

Table 4. Electron microprobe mean analyses (wt%) for the garnet and saponite in Beds 4 and 8 with standard deviation, σ, (in parenthesis). Lower table shows mineral formulae calculated on the basis of O_{24} for garnet and $O_{20}(OH)_4$ for saponite.

Figure 1. Location map for Lòn Ostatoin.

Figure 2. Photograph of the Lòn Ostatoin exposure including sample locations. Note the deformation and tilting upwards of the sedimentary rocks at the south-eastern end of the exposure. Samples CA13, 16, 17, 20, 21, 24 and 25 were all removed from Bed 8. Sample CA32, from the stratigraphically lower Bed 4, is not shown but is located approximately 50 m north-east of this view. Saponite concentration decreases north-westwards from this outcrop.

Figure 3. Composite section of the Kilmaluag Formation, Lòn Ostatoin (based on data from Andrews 1984).

Figure 4. Whole-rock X-ray diffraction trace for a sample from Bed 8 compared to the International Centre for Diffraction Data (ICDD) standard 'stick' patterns for grossular and saponite.

Figure 5. Scanning electron photomicrographs of metasomatized limestone features. (a) Typical morphologies of the grossular garnet crystals (gr) and saponite clay matrix (sa). Sample CA17, Bed 8. (b) Corroded, euhedral grossular garnet (gr). Sample CA17, Bed 8. (c) Low magnification backscattered image showing abundant, uniformly-sized grossular crystals. Large bioclasts have been replaced by apatite (ap). Sample CA32, Bed 4. (d) Backscattered image showing euhedral grossular crystals (gr), commonly with cracks and corroded cores. Sample CA32, Bed 4. (e) Backscattered image of saponite clay matrix (sa). Sample CA32, Bed 4.

Figure 6. Air-dried and ethylene glycol-solvated <2 μm oriented mount X-ray diffraction traces for a sample from Bed 8. The saponite basal (d_{00l}) spacings and most intense peaks for other phases are indicated.

Figure 7. North American Shale Composite (NASC)-normalised element diagram for limestone samples from Beds 4 and 8.

Figure 8. Backscattered scanning electron photomicrographs of metasomatized mudstone features. (a) Laminated mudstone with sporadic subrounded, silt-sized quartz and feldspar grains. The dark laminae are cemented by analcime (an). Sample CA15, Bed 5. (b) Bioclast with analcime-replaced core (an) and apatite-replaced exterior (ap). Sample CA14, Bed 7. (c) Vein of analcime (dark grey, an) overgrowing euhedral, coarse-grained clinoptilolite crystals (light grey, cl). Sample CA19, Bed 7. (d) Detrital quartz (qz) and feldspar (fd) grains cemented by clinoptilolite (cl) in a silty lamina. Sample CA18, Bed 9.

Figure 9. North American Shale Composite (NASC)-normalised element diagram for mudstone samples from Beds 5, 7 and 9.

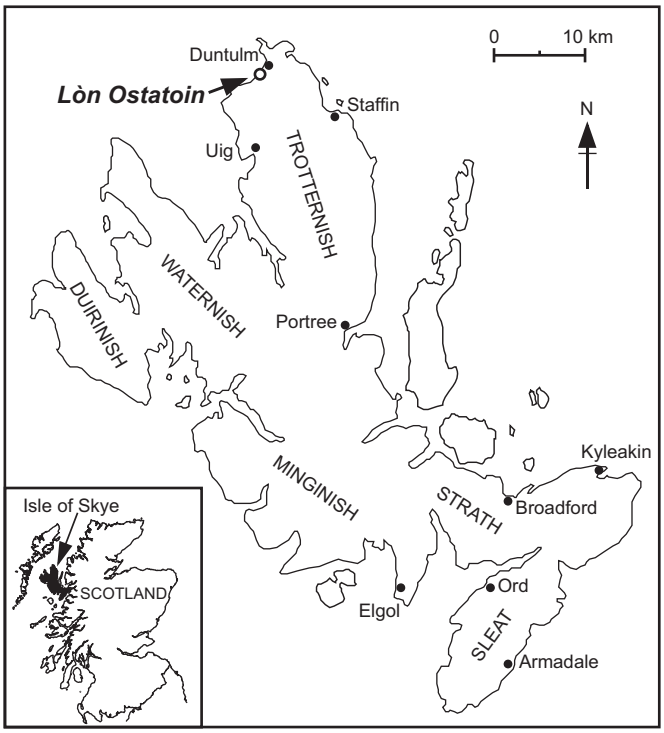

Kemp et al
Figure 01

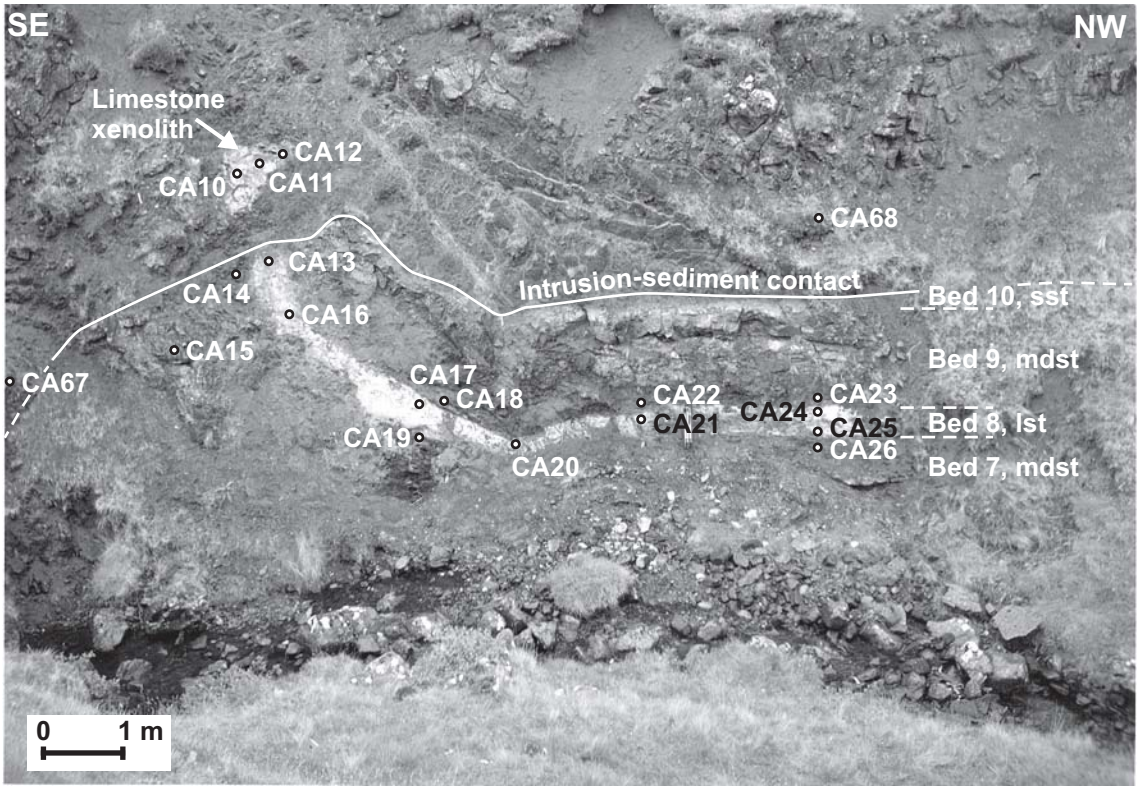

Kemp et al
Figure 02

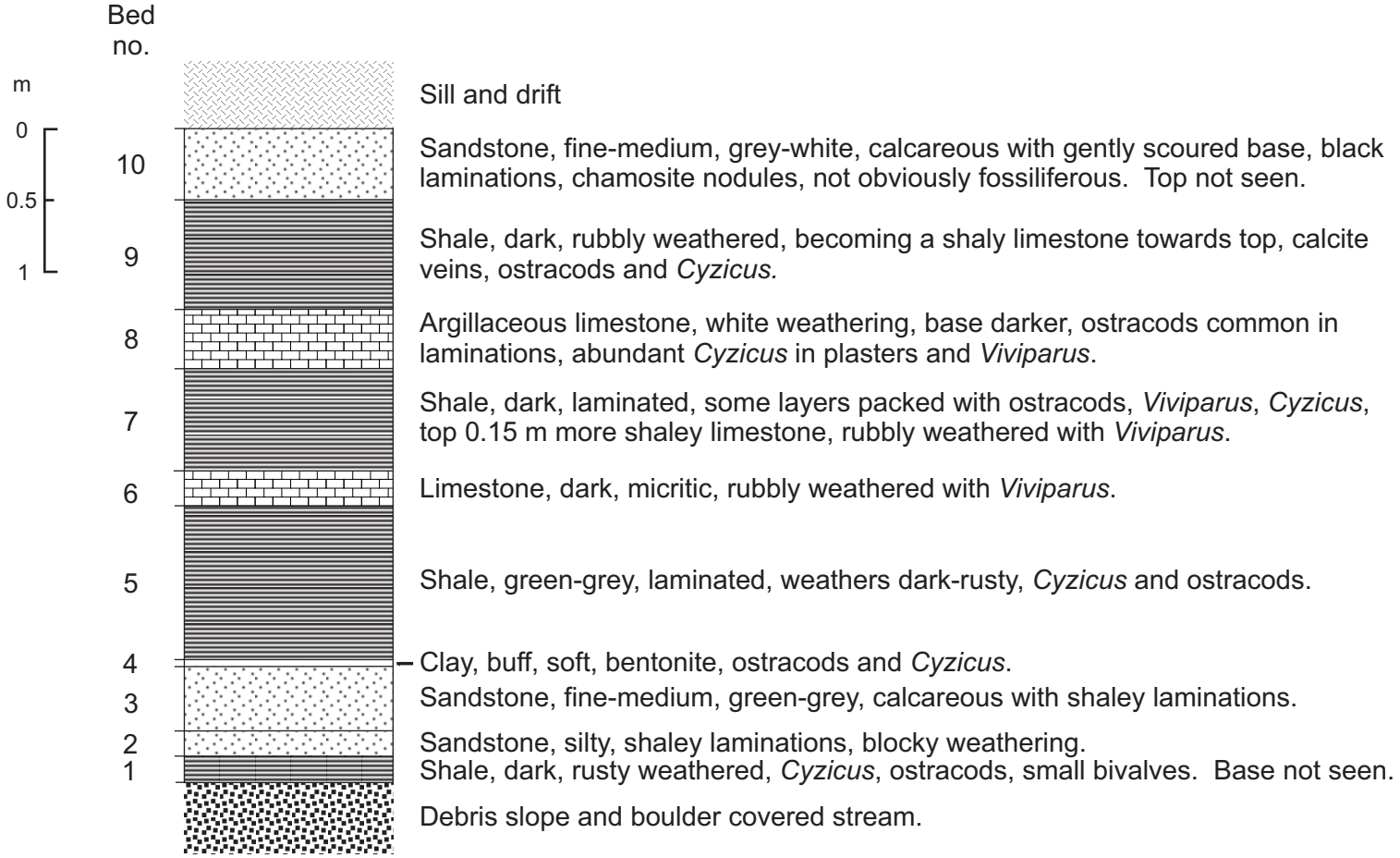

Kemp et al
Figure 03

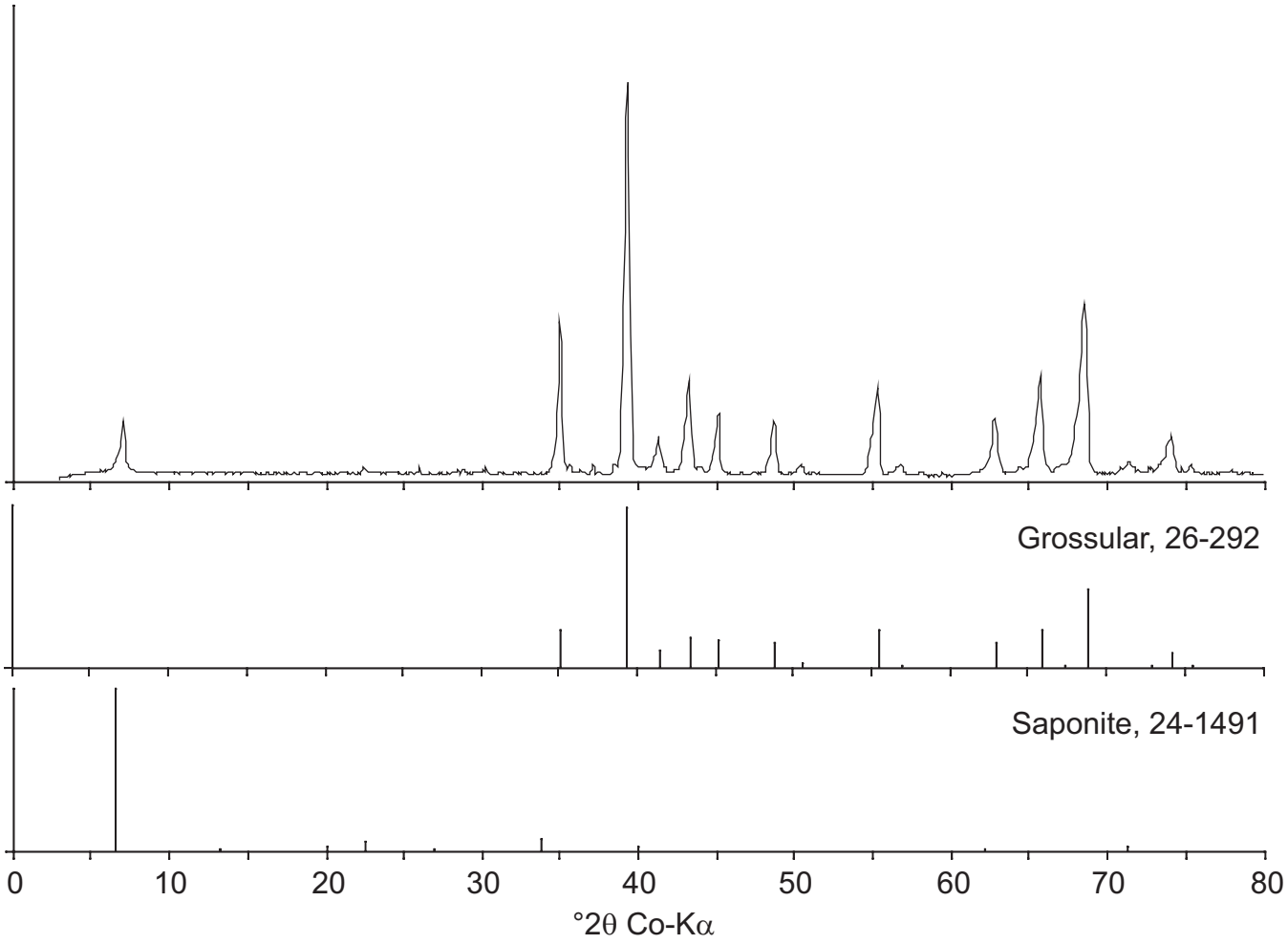

Kemp et al
Figure 04

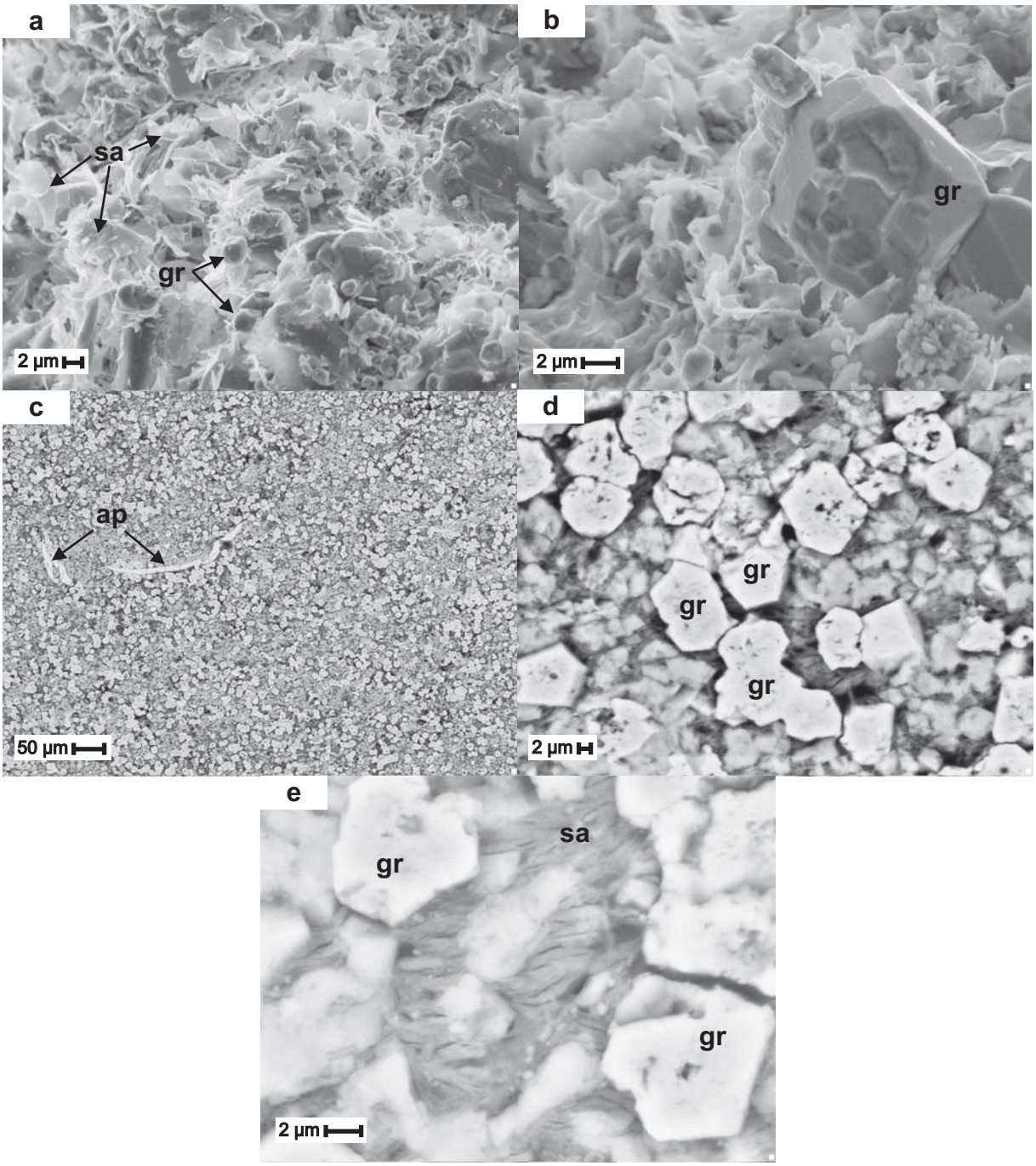

Kemp et al
Figure 05

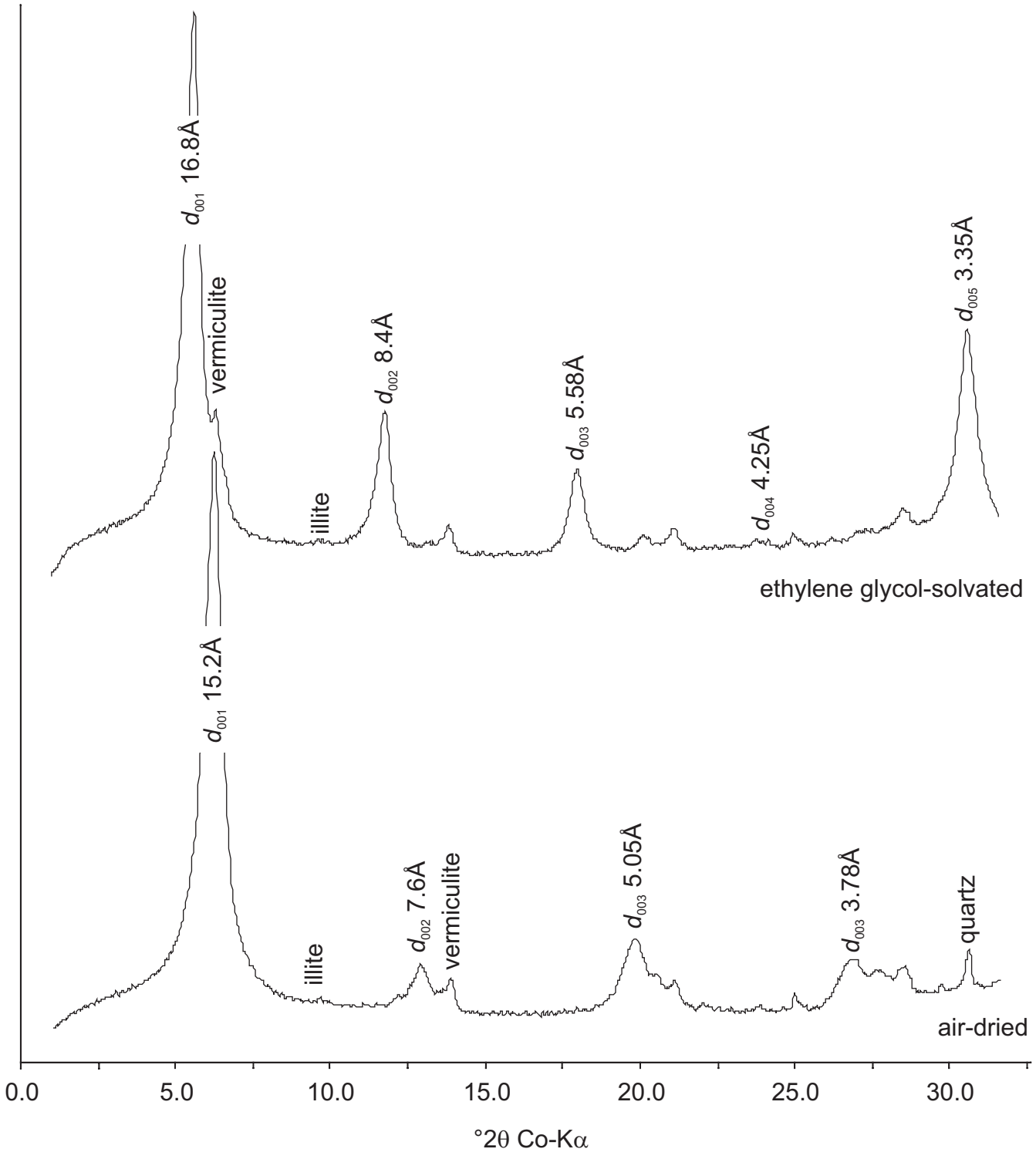

Kemp et al
Figure 06

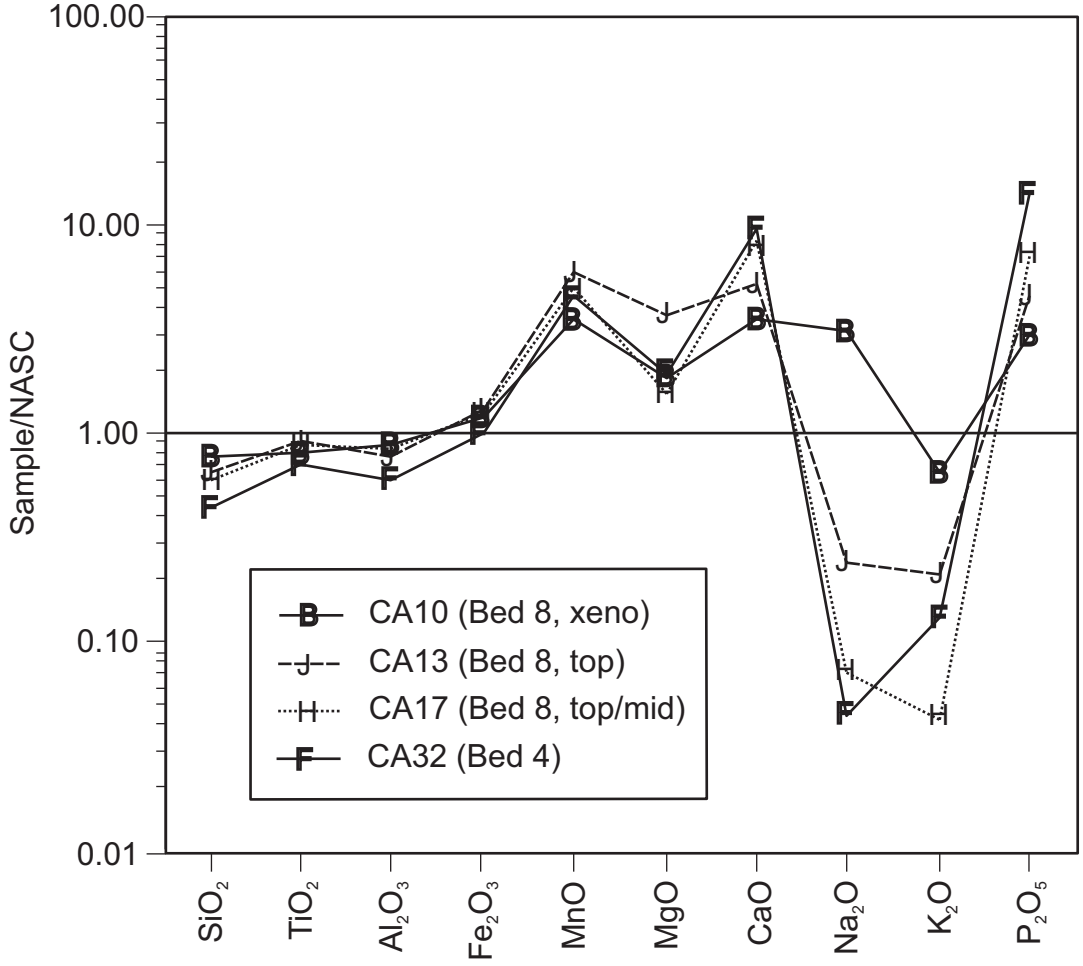

Kemp et al
Figure 07

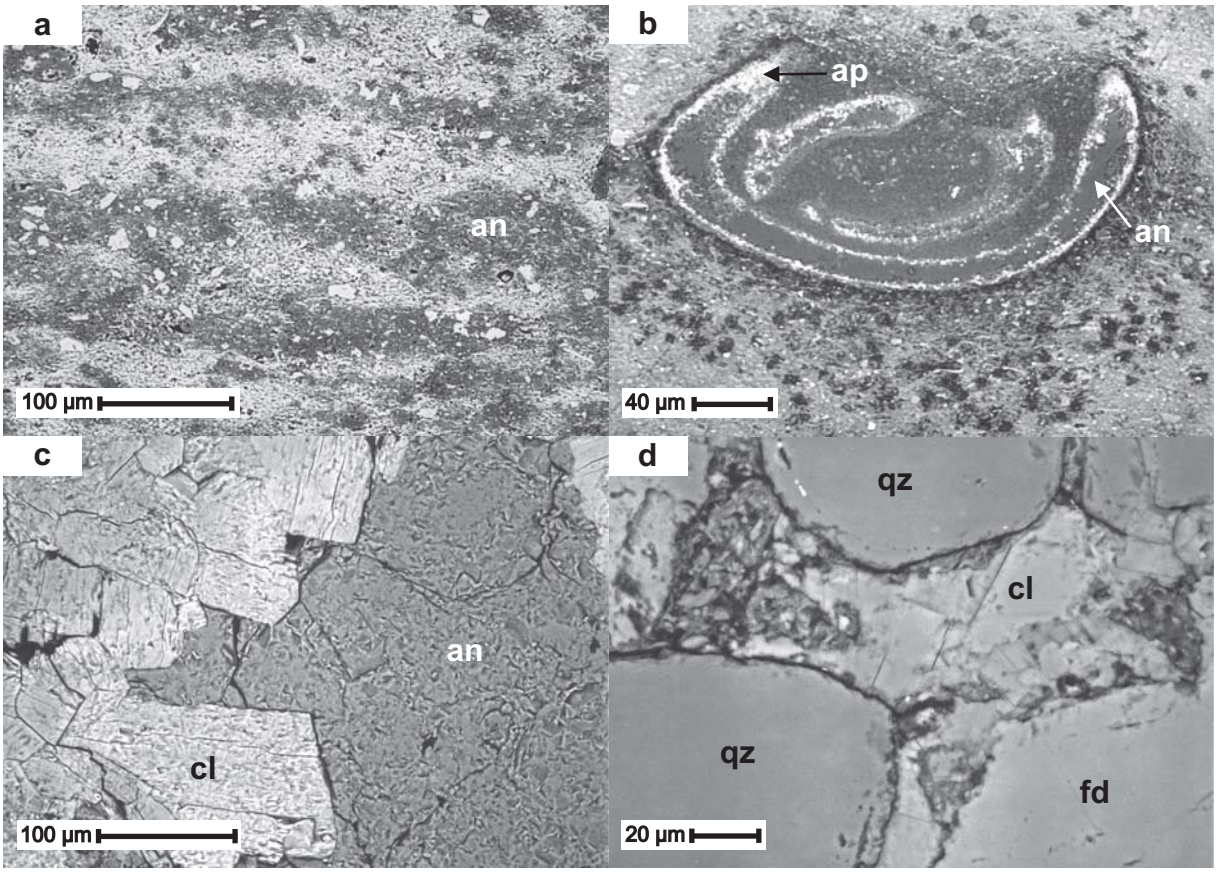

Kemp et al
Figure 08

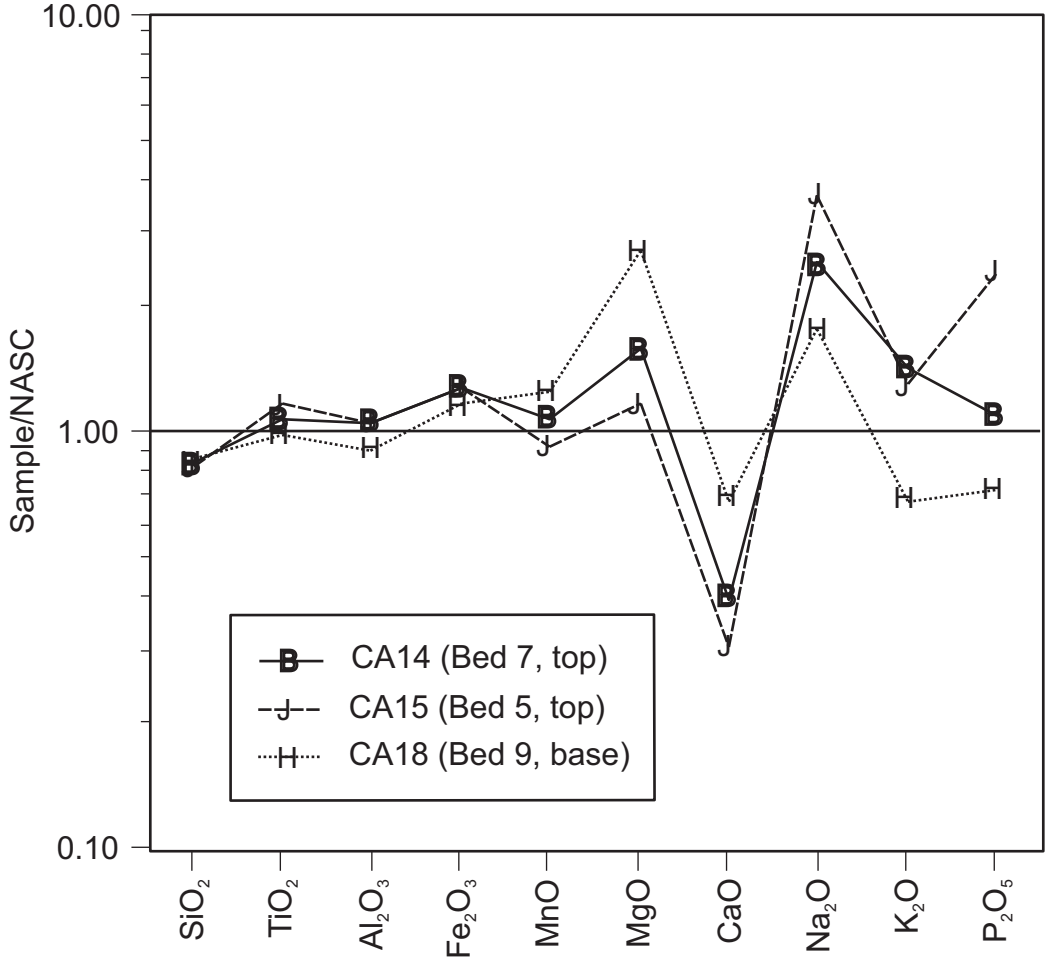

Kemp et al
Figure 09